THE INFLUENCE OF INITIAL STRESS ON THE SIZE EFFECT OF CONCRETE FLEXURAL STRENGTH

(Translation from Journal of Materials, Concrete Structures and Pavements of JSCE, No. 550/V-33, pp. 85-94, November 1996)

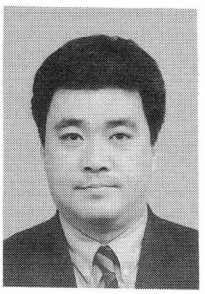

Junichiro NIWA

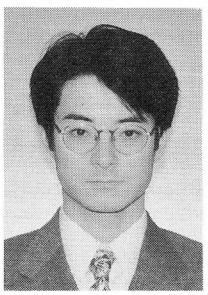

Shigenori HIDAKA

Tada-aki TANABE

To clarify the influence of drying-shrinkage induced initial stress in concrete on the size effect of flexural strength, the initial stress of concrete specimens was measured and the stress distribution was evaluated experimentally. As the initial stress distribution changes with the dimensions of the specimen and drying period, it is considered inappropriate to model the stress distribution with a second-order polynomial. Further, time-dependent changes in material properties were also evaluated by experiment. Based on fracture mechanics and incorporating this information, the influence of initial stress on the size effect of concrete flexural strength was calculated and the results were also confirmed by experimental data. According to this investigation, it is clear that the influence of initial stress becomes significant as the ratio of specimen size to characteristic length of concrete increases.

Keywords: *flexural strength, size effect, initial stress, drying shrinkage, fracture mechanics, material property*

Junichiro NIWA is an associate professor of civil engineering at Nagoya University, Japan. He received his Doctor of Engineering degree from the University of Tokyo. He specializes in the mechanics of concrete structures including fracture mechanics and nonlinear finite element analysis.

Shigenori HIDAKA is a design engineer at P.S. Corporation, Japan. He received his Master of Engineering degree from Nagoya University in 1995. He is now working on the design and construction of prestressed concrete bridges.

Tada-aki TANABE is a professor of civil engineering at Nagoya University, Japan. He received his Doctor of Engineering degree from the University of Tokyo. He is chairman of the JCI Committee on the Thermal Stress of Massive Concrete Structures besides being a member of various committees of the JSCE, JCI, IABSE, and RILEM.

1. INTRODUCTION

In reinforced concrete members, the concrete flexural strength is generally used to predict the flexural cracking moment, or the flexural rigidity of the reinforced concrete member after cracking. However, in concrete without reinforcement, or in reinforced concrete with a very low reinforcement ratio such as used in extremely large structural members, the flexural strength of the concrete is also required to estimate the actual capacity of the structural member itself.

As studies of fracture mechanics of concrete have progressed, it has become clear that flexural strength should not be adopted as a material property of concrete. Flexural strength is dependent on the size of the specimen, so even with specimens made from the same concrete, particularly from concrete with the same tensile strength and fracture properties, their flexural strength would gradually decrease with increasing specimen height. In other words, it is clear that there is a significant size effect on flexural strength. As a result of this size effect, the concrete flexural strength cannot be used as a material property of concrete.

In direct tensile strength tests, since crack propagation conditions are not completely uniform, the tensile strength is affected by the bending itself. Therefore, strictly speaking, there is a size effect on tensile strength, but the influence is small in comparison with that on flexural strength; thus, tensile strength is used as a material property that has no size effect in this paper.

The characteristic value of flexural strength for design is specified in the JSCE's Standard Specification for Design and Construction of Concrete Structures. In the Specification, the use of a standard specimen having a height of 10 cm to 15 cm is implicitly assumed. On the other hand, CEB-FIP Model Code 90 [1] gives the following design equation for the estimation of flexural strength, in which the size effect is taken into account through a function of the height of the specimen:

$$\frac{f_b}{f_t} = \frac{1 + 1.5\,(h/h_o)^{0.7}}{1.5\,(h/h_o)^{0.7}} \tag{1}$$

Where, f_b : flexural strength of concrete; f_t : tensile strength of concrete; h : height of beam and h_o = 10 cm.

Further, Uchida, et al. proposed the following equation for predicting the size effect based on the height of a beam and the concrete characteristic length [2].

$$\frac{f_b}{f_t} = 1 + \frac{1}{0.85 + 4.5\,(h / l_{ch})} \tag{2}$$

Where, l_{ch} : concrete characteristic length defined as follows using the fracture energy G_F of concrete, Young's modulus E_c, and tensile strength f_t.

$$l_{ch} = E_c\, G_F \,/\, f_t^{\,2} \tag{3}$$

The authors also carried out a parametric study on the flexural strength of a concrete beam subjected to four-point bending, using finite element analysis based on fracture mechanics, and as a result proposed the equation below for predicting the size effect on flexural strength [3]. In this equation, the height of a beam and the compressive strength of concrete, f_c', are intentionally used instead of the characteristic length, l_{ch}, to predict the size effect.

$$\frac{f_b}{f_t} = 1.36\,(h/h_o)^{-\frac{1}{6}}\,(f_c'/f_{co}')^{-\frac{1}{20}} \qquad (4)$$

Where, $f_b/f_t \geqq 1.0$, h_o = 10 cm, f_{co}' = 300 kgf/cm^2.

The above equations differ somewhat from each other, but they all predict a similar size effect of concrete flexural strength [3]. However, they are based on the assumption that there is no initial stress within the concrete beam. It is generally thought that the existence of initial stress resulting from drying shrinkage has a significant influence on flexural strength, and so must be taken into account in any study of the size effect. In this investigation, the extent to which the existence of initial stress due to drying shrinkage influences the size effect of concrete flexural strength is experimentally and numerically investigated.

2. INITIAL STRESS OF CONCRETE DUE TO DRYING SHRINKAGE

2.1 Purpose of Initial Stress Measurements

Tazawa, et al. measured the drying-shrinkage induced stress distribution within concrete using the successive layer-cutting method, and then modeled the results with a second-order polynomial curve [4]. On the other hand, Akita, et al. analytically indicated that tensile stress resulting from drying shrinkage is generated only in a layer from the dried surface to around 1 cm in depth [5].

As illustrated by this, a variety of analytical methods have been proposed regarding the magnitude and distribution of initial stress inside concrete. It is easy to predict that the existence of initial stress will have a significant influence on concrete flexural strength. Thus, in numerical analysis based on fracture mechanics, it is necessary to incorporate the influence of initial stress if the analytical results are to be made more realistic. In this study, the method used by Tazawa, et al. will be used to determine the magnitude and distribution of initial stress by the successive layer-cutting method. In consideration of future application to size effect analysis, relatively large specimens will be tested along with small ones.

2.2 Stress Measurement Theory

A conventional procedure for stress measurement [6] was applied based on the successive layer-cutting method. As shown in Figure 1, when an initial tensile stress exists on both surfaces of an elastic plate and there is initial compressive stress within the plate, layers of the plate are cut off one after another. As a result, the axial tensile force and flexural moment generated by tensile stresses in this cut-off portion, have to be borne by the remainder; as a

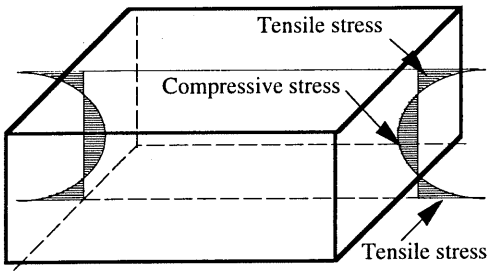

Figure 1. Conceptual Diagram of Initial Stress Distribution within an Elastic Plate

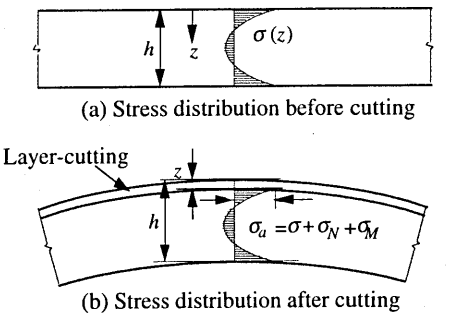

Figure 2. Stress Distribution and Deformation of Plate before and after Layer-Cutting

result, the total length of the plate increases, and the plate curves upward in a convex shape. At that moment, from measurements of strain in the remainder, the change in curvature is clarified to obtain the initial stress in the portion removed. In this case, the magnitude of the initial stress must be within the elastic range. The theory behind these measurements is briefly explained below.

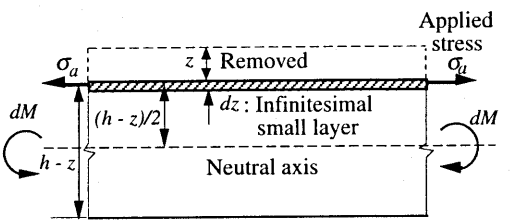

Figure 3. Flexural Moment Applied to dz

As shown in Figure 2, a situation where a layer at level z is removed from the surface of a plate having a height h and unit width $b = 1$ is considered. The initial stress existing in this portion is indicated as $\sigma = \sigma(z)$ and after cutting, when the stress at level z changes to σ_a, the stress increase is separated into σ_N resulting from axial tensile force and σ_M resulting from flexural moment, as indicated in Eq. (5).

$$\sigma_a = \sigma + \sigma_N + \sigma_M \tag{5}$$

The equilibrium of axial force before and after cutting, and the relationship between moment acting on the cross section and the curvature after cutting, allow σ_N and σ_M to be calculated respectively using Eqs. (6) and (7).

$$\sigma_N = \int_0^z \sigma(z)\, dz / (h - z) \tag{6}$$

$$\sigma_M = \frac{E}{\rho} \frac{h - z}{2} \tag{7}$$

In these equations, E is Young's modulus and $1/\rho$ is the curvature of the plate after cutting.

In order to consider the change in stress σ_a after cutting, we consider that a layer of dz has been removed from level z. The flexural moment generated by the stress on this dz portion is indicated as Eq. (8), with reference to Figure 3.

$$dM = \sigma_a \frac{h - z}{2} dz = \frac{\sigma_a (h - z)}{2} dz \tag{8}$$

Further, from $1/\rho = M/(EI)$, the following equation is obtained:

$$d\left(\frac{1}{\rho}\right) = \frac{dM}{EI} = \frac{1}{EI} \frac{\sigma_a (h - z)}{2} dz = \frac{6\sigma_a}{E (h - z)^2} dz \tag{9}$$

So, σ_a is given by the following equation as a derivative of the curvature:

$$\sigma_a = \frac{E (h - z)^2}{6} d\left(\frac{1}{\rho}\right) / dz \tag{10}$$

From equations (5), (6), (7), and (10), we get Eq. (11).

$$\frac{E (h - z)^2}{6} d\left(\frac{1}{\rho}\right) / dz - \frac{E}{\rho} \frac{(h - z)}{2} - \int_0^z \sigma (z)\, dz / (h - z) = \sigma \tag{11}$$

Since Eq. (11) contains σ in both sides, calculation would be complicated. Therefore, Eq. (11) is rewritten with σ indicated as a function of the curvature. Equation (11) is then differentiated with respect to z, and is further partially integrated and rearranged to finally obtain Eq. (12) [6].

$$\sigma = \frac{E (h - z)^2}{6} d\left(\frac{1}{\rho}\right) / dz - \frac{2E (h - z)}{3} \frac{1}{\rho} + \frac{E}{3} \int_0^z \frac{1}{\rho} dz \tag{12}$$

The right-hand side of Eq. (12) can be estimated through the curvature $1/\rho$ and both its derivative and integral. Therefore, if the change in curvature due to layer-cutting is measured and the relationship between z and $1/\rho$ is experimentally clarified, the distribution of initial stress in the plate is obtained.

2.3 Outline of Test Specimens

The specimens used for measurements of initial stress are illustrated in Figure 4. They are 20-cm or 50-cm square concrete plates of 10 cm thickness, and are designed to simulate the equal moment region of a plain concrete beam subjected to four-point loading as shown in Figure 5.

Based on the measurement method explained in 2.2, the initial stress will be obtained by cutting away layers one after another. In the experiments, 30-mm-long strain gauges were attached on the surface of the specimen at 2.5-cm pitch when the layers were cut off. A concrete cutter could not be used, since this would introduce heat and water which would have an influence on the

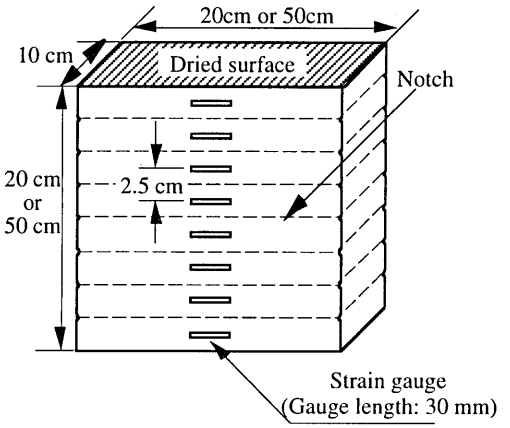

Figure 4. Specimens for Initial Stress Measurements

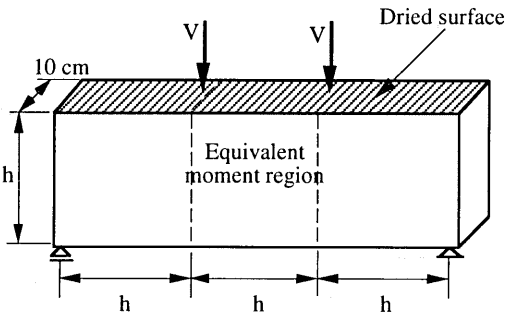

Figure 5. Plain Concrete Beam Subjected to Four-Point Loading

distribution of initial stress. Therefore, layer-cutting was carried out by the splitting method. In order to accurately determine the position at which a specimen would part, notches in the shape of right isosceles triangles with 1-cm sides were formed at 2.5-cm intervals, as shown in Figure 6. To remove each successive layer, a 16-mm round bar was placed in the notch on each side of the specimen and force applied to cause a split at the predetermined point.

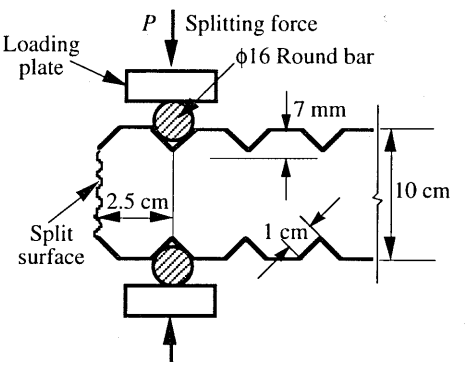

Figure 6. Notches in Specimen and Splitting Method

Three specimens were prepared for each experimental condition. To prevent drying shrinkage, the surface of the concrete was covered with a polyvinyliden chloride sheet (vinyl chloride sheet) immediately after casting; the mold was removed 24 hours after casting and the concrete specimen was cured in water for 7 days.

The concrete was then left in air (25±3℃, 70±5%RH). Only the upper and lower surfaces of each specimen were dried. Rubber-type adhesive tape 0.55-mm thick, a vinyl chloride sheet, and cloth adhesive tape were affixed to the undried sides of the specimen. Seams in the vinyl chloride sheet were securely sealed with polyester tape. At 3 days, 7 days, 28 days, and 91 days after drying started, layers were cut off and initial stress due to drying shrinkage was calculated.

The mix proportion of the concrete used in the test is shown in Table 1. High-early-strength cement (specific gravity : 3.14) was used; Kasugai crushed stone having a maximum diameter of 13 mm and specific gravity of 2.62 was used as the coarse aggregate; the water absorption ratio was 0.86% and F.M. was 6.62. Toyota mountain sand having specific gravity of 2.51, water absorption ratio of 1.47%, and F.M. of 2.80 was used as the fine aggregate. An appropriate amount of super plasticizer was added to obtain a slump of about 8 cm.

Table 1. Mix Proportion of Concrete

W/C (%)	s/a (%)	Unit weight (kg/m^3)				
		W	C	S	G	SP
50	48.5	191	382	796	886	0.43

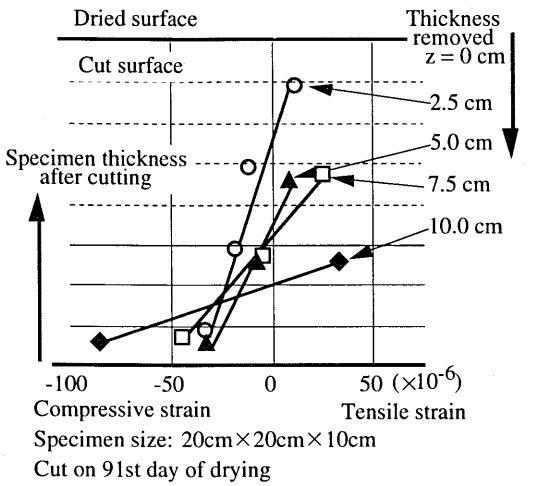

Figure 7. Strain Distribution Resulting from Layer-Cutting

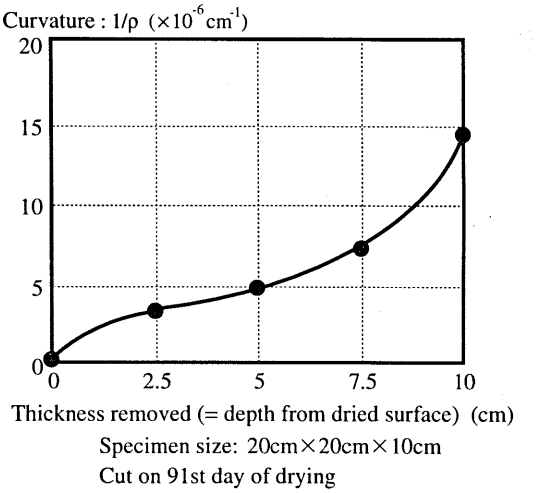

Figure 8. Change in Curvature of Concrete Plate due to Layer-Cutting

2.4 Initial Stress Measurement Results

Based on the stress measurement method described in 2.2, the strain caused by layer-cutting was measured. The strain distribution shown in Figure 7 is the measured result for one of the 20-cm square specimens cut at 91 days. In this study, it is assumed that the distribution of initial stress between the upper and lower dried surfaces would be symmetrical, so layer-cutting was stopped at half height. Since the number of remaining strain gauges falls as cutting proceeds, it is considered that further cutting does not provide any useful information.

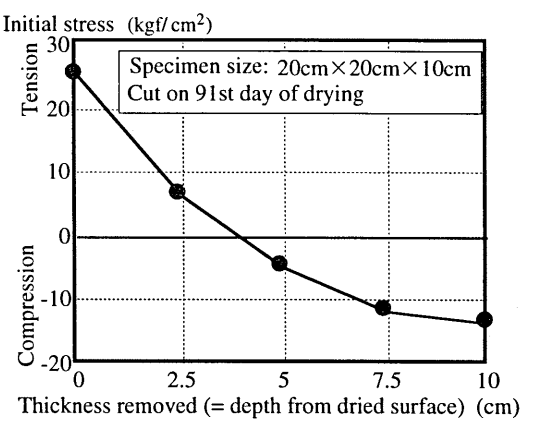

Figure 9. Initial Stress Distribution Found by Layer-Cutting

As shown in Figure 7, the experimentally obtained strain values indicate almost a linear distribution, and in specimens after layer-cutting it can be judged that the plane section would remain plane. This strain distribution is approximated by a regression line using the method of least squares. Based on this regression line, the change in curvature due to layer-cutting is experimentally determined.

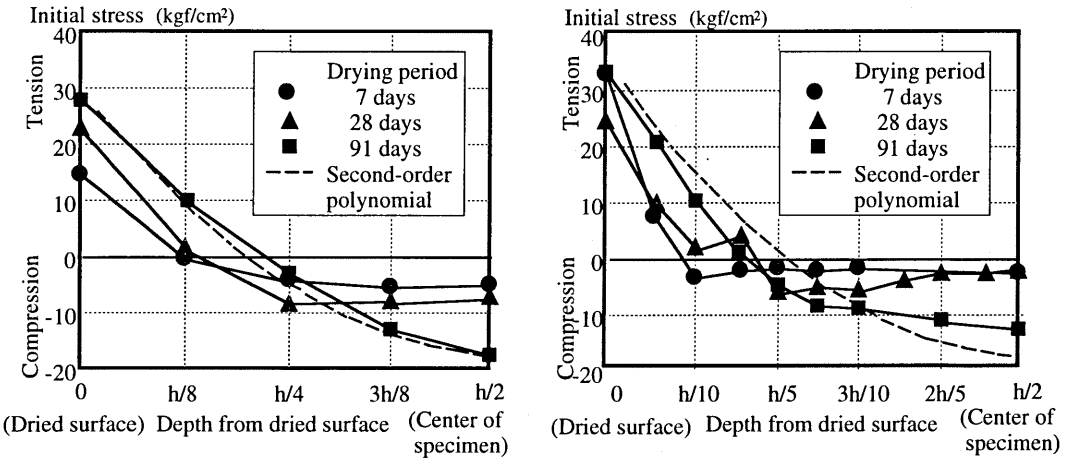

(a) Initial stress distribution for specimen of 20 cm

(b) Initial stress distribution for specimen of 50 cm

Figure 10. Measured Initial Stress Distributions

Figure 8 shows the change in curvature due to layer-cutting based on the strain distribution obtained from Figure 7. The curve shown in Figure 8 was drawn by modeling the plotted points with a polynomial expression (fourth order, in this case). The derivative of curvature which is required in Eq. (12) is determined from the tangent of the curve in Figure 8, and the integral of the curvature is determined as the area below the same curve. Finally, the initial stress was calculated using Eq. (12). Figure 9 shows an example of the distribution of initial stress as obtained by this method (for a specimen 20 cm × 20 cm × 10 cm and a drying period of 91 days).

When calculating initial stress by Eq. (12), Young's modulus of the concrete is required in addition to the change in curvature. In this study, based on compression tests on cylindrical specimens (ϕ10 × 20 cm) under the same environmental conditions as the plate-shaped specimens, Young's modulus was measured and substituted into Eq. (12).

Figures 10 (a) and (b) show the shape of the measured initial stress distribution for specimens of 20-cm square and 50-cm square, respectively. To make the comparison easier, the horizontal axis is a nondimensional scale obtained by dividing the distance from the dried surface by the length of the side of the specimen. The dotted line is a second-order polynomial curve for reference. In this curve, the measured initial stress on the drying surface of the specimen of 91 days after the start of drying is given as the boundary condition.

From the distribution of initial stress in a relatively small 20-cm square specimen as shown in Figure 10 (a), it was recognized that tensile stress on the drying surface increases, and the point at which the stress changes from tension to compression gradually moves toward the center of the specimen as the drying period increases. At 28 days after drying starts, rapid stress increase is limited to the volume near the drying surface, and the distribution of initial stress within the specimen is almost uniform. Therefore, in this case, it is not appropriate to model the distribution of initial stress as a second-order polynomial curve. However, at 91 days, the shape of the distribution almost coincides with a second-order polynomial curve.

On the other hand, there is a significant difference in the case of a relatively large specimen of 50-cm square, as shown in Figure 10 (b). The surface tensile stress increases as the drying period becomes longer, and the stress turning point also moves toward the center of the specimen, but the results are quite different from those for the 20-cm square specimen. For example, in the case of a 91-day drying period, the area with significant tensile stress is limited to that near the drying surface; it is clear that in order to model the distribution of initial stress as a second-order polynomial curve, an additional period of drying is required. In addition to this confinement of tensile stress to the area near the drying surface in a 50-cm square specimen dried for 91 days, the compressive stress distribution in the center portion is almost uniform, and its magnitude is smaller than that in a 20-cm square specimen. This tendency is expected to become more significant as the specimen becomes larger. Therefore, except when the specimen is small and the drying period is sufficiently long, it is judged inappropriate to model the distribution of initial stress as a second-order polynomial.

3. TIME-DEPENDENT CHANGE IN MATERIAL PROPERTY OF CONCRETE

3.1 Outline of Test

The ultimate target of this study is to clarify the extent to which the size effect of concrete flexural strength is influenced by initial stress resulting from drying shrinkage. To do this, the layer-cutting test described in Chapter 2 was carried out to obtain data on the distribution of initial stress. However, in order to predict flexural strength through numerical analysis, a number of material properties such as tensile strength, elastic modulus, and fracture energy are required in addition to the distribution of initial stress. How these material properties change with increasing specimen age was clarified through experiments.

The materials and mix proportion of the concrete were the same as those used in the measurement of initial stress (Table 1). Compressive strength, tensile strength, and Young's modulus were obtained using ordinary cylindrical specimens ($\phi 10 \times 20$ cm). Young's modulus was determined from the 1/3 secant modulus of the peak stress on the stress-strain curve. Fracture energy G_F was determined based on the method recommended by RILEM, using a three-point bending test on a notched beam specimen with dimensions 10 cm $\times$ 10 cm $\times$ 84 cm.

Three or more specimens were prepared for each test condition, and a mean value was calculated. Until 7 days, all specimens were cured in water; after that, some were dried freely in air (25 ± 3℃, 70 ± 5%RH), and some were kept in water. This was done to investigate the degree of influence of drying shrinkage on time-dependent changes in material properties.

3.2 Time-Dependent Changes in Material Properties of Concrete

Figure 11 shows the time-dependent changes in compressive strength, tensile strength, elastic modulus, and fracture energy. Solid lines in Figure 11 refer to specimens dried in air after water curing; broken lines refer to specimens cured only in water.

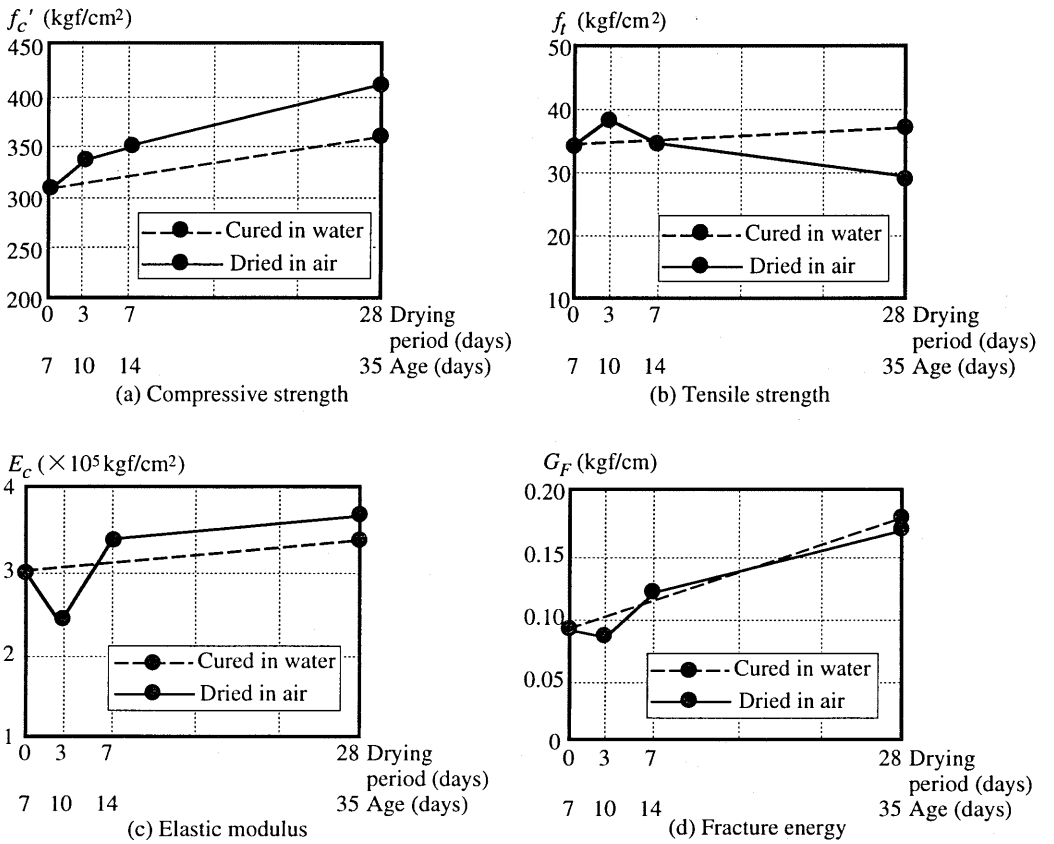

Figure 11. Changes in Material Properties of Concrete with Time

It was found that the compressive strength of specimens increases gradually with time whether subjected to drying in air or to curing in water. However, the amount of this increase is larger in dried specimens. The tensile strength of dried specimens and those cured in water differs. The tensile strength of specimens cured in water gradually increases, as does compressive strength, but in the case of dried specimens it shows a sudden increase after the start of drying before gradually decreasing. The trends in time-dependent changes in elastic modulus and fracture energy are similar; in the case of curing in water, both gradually increase. However, in the case of drying, they suddenly decrease after the start of drying, then increase again, and at 28 days, they are almost the same in magnitude as for the specimens cured in water.

4. TIME-DEPENDENT CHANGES IN FLEXURAL STRENGTH OF CONCRETE

4.1 Outline of Test

In order to examine the influence of initial stress on concrete flexural strength, experiments were carried out in which the dimensions of specimens and curing conditions were changed. The materials and mix proportion of the concrete were the same as those used previously (Table 1). Plain concrete beams of three different sizes were manufactured: height 10 cm × width 10 cm

× length 40 cm (span: 30 cm); height 20 cm × width 10 cm × length 70 cm (span: 60 cm); height 50 cm × width 10 cm × length 180 cm (span: 150 cm). The flexural strength of the concrete was determined by carrying out four-point bending tests on the above specimens.

All specimens were cured in water for 7 days; then, some were kept in water, and some were dried in air (25±3℃, 70±5%RH) with the four side surfaces (except the upper and lower surfaces) sealed in the same manner as for the measurement of initial stress.

4.2 Test Results

Figure 12 shows the time-dependent changes in concrete flexural strength. Test results are indicated by the ● mark in Figure 12. Three each of 10-cm and 20-cm high beam specimens were prepared for each test condition, and the mean values were calculated. In this case, the flexural strength of the specimens cured in water noticeably increased with time. On the contrary, the flexural strength of specimens dried in air after water curing suddenly decreased after the start of drying for a period of 3 to 7 days; thereafter, it increased again and, at 28 days, reached almost the same level as that of specimens cured in water.

One 50-cm high beam specimen was continuously cured in water; two others were dried for 7 or 28 days, for a total of three specimens. Although the number of specimens was not really sufficient, no recovery of flexural strength with increased drying period was observed in these specimens, unlike the 10-cm high and 20-cm high specimens. Further, flexural strength tended to decrease gradually as the drying period became longer, and was apparently smaller in comparison with that of specimens cured in water.

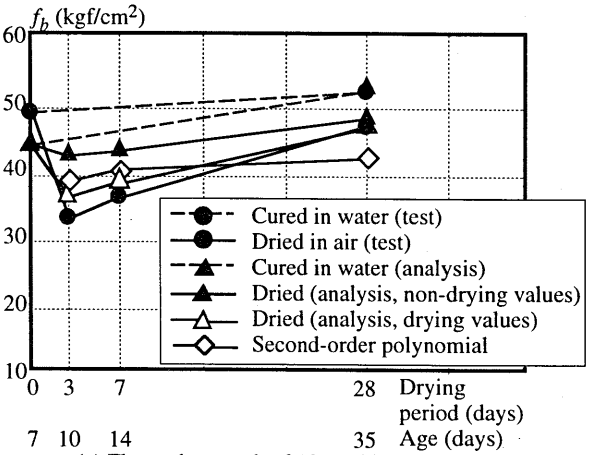

(a) Flexural strength of 10-cm high beam

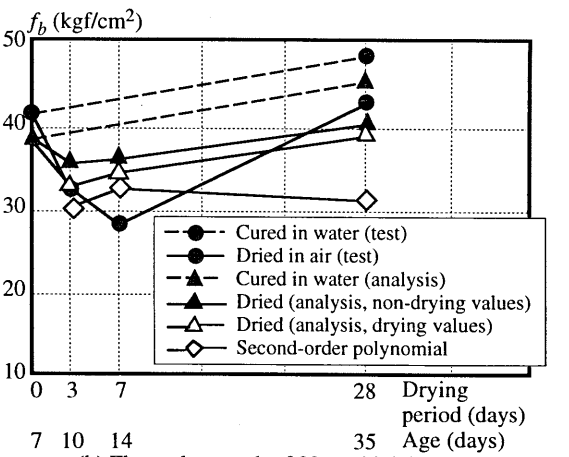

(b) Flexural strength of 20-cm high beam

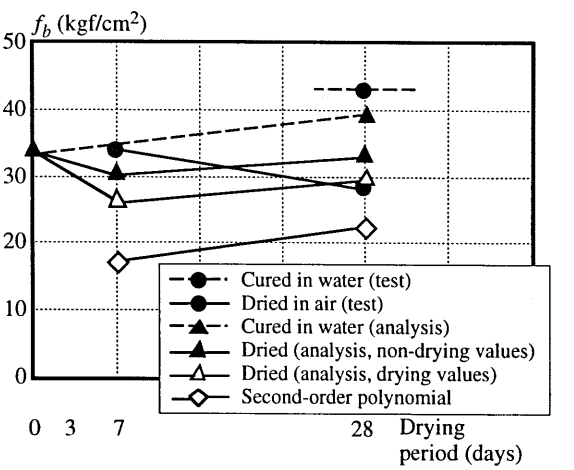

(c) Flexural strength of 50-cm high beam

Figure 12. Changes in Flexural Strength of Concrete with Time

4.3 Analytical Results

The △ and ▲ marks in Figure 12 represent the results of finite element analysis with a fictitious crack model and nonlinear rod elements based on fracture mechanics. The experimental results given in Figure 10 are used directly as the initial stress distribution of the dried specimen. In the case of a 10-cm high specimen, the nondimensional initial stress distribution obtained from a 20-cm high specimen is used in the direction of specimen height. Material properties such as fracture energy and tensile strength, which are adopted for the analysis, are the test results shown in Figure 11.

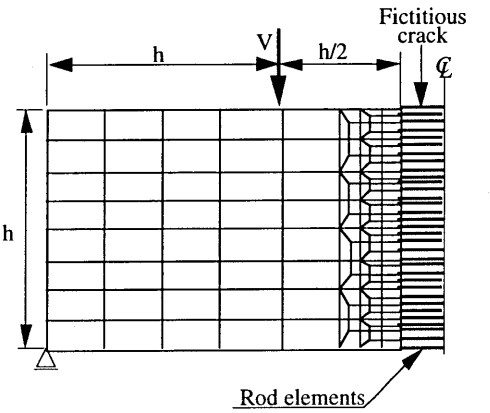

Figure 13 Mesh Discretization for Finite Element Analysis

Figure 13 shows the finite element mesh discretization used for the analysis. Only one-half of a beam is analyzed since it was assumed to be symmetrical. A fictitious crack is assumed in the center of the span and 33 rod elements [7] are placed in a direction perpendicular to the fictitious crack. Each rod element has a unit length (in this case, because half of the beam is analyzed, the rod element length is L = 1/2), and the 1/4 tension softening model is used for the tension softening curve. All other concrete elements are assumed to be elastic, and are modeled by four-node isoparametric elements. The initial stress and material properties are taken into account in the formulation of the rod elements.

In Figure 12, analytical results for material properties under drying conditions are indicated by △, and those for specimens cured only in water are indicated by ▲. In the analysis of the material properties of dried specimens (△), the effect of drying is considered as double in the evaluation of the distribution of initial stress and of material properties. Thus, although it is considered more appropriate to use material properties without the effect of drying (i.e. when the specimen is cured in water (▲)), analytical results of material properties of dried specimens (△) are closer to the test results.

As shown in Figure 12, for beams with heights of 10 cm and 20 cm, the analytical results taking into account the distribution of initial stress due to drying and time-dependent changes in material properties reflect the decrease in flexural strength and its recovery as observed in the tests.

Similar analytical results are indicated by ◇ in Figure 12 for cases where the shape of the initial stress distribution is assumed to be a second-order polynomial curve. In this case, although a decrease in flexural strength immediately after the start of drying is predicted, its subsequent recovery is not properly modeled. This indicates that it is necessary to correctly evaluate the shape of the initial stress distribution in the cross-section as well as the time-dependent changes in material properties in order to predict the time-dependent changes in flexural strength; giving proper consideration to both makes it possible to predict the time-dependent

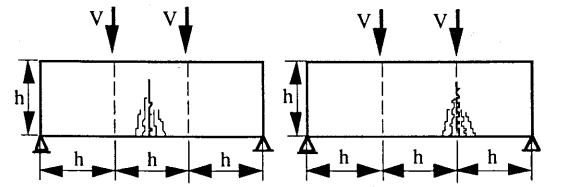

(a) Fracture of beam at 7 days after start of drying (b) Fracture of beam at 28 days after start of drying

Figure 14. Crack Propagation at the Ultimate State in 50-cm High Beam

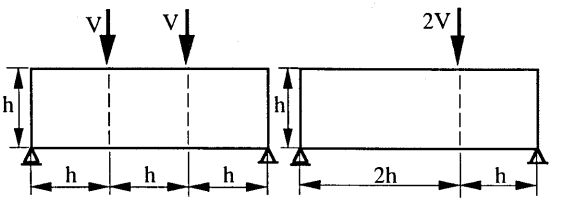

(a) Four-point loading (b) Eccentric loading

Figure 15. Difference in Loading Conditions

changes in flexural strength through numerical analysis based on fracture mechanics.

In a 50-cm high beam, the analytically obtained trend of time-dependent changes in flexural strength is, qualitatively speaking, the same as for beams with heights of 10 cm and 20 cm. Figure 14 shows crack propagation in a 50-cm high beam at the ultimate state as obtained from the experiment.

In the test, four-point loading was applied using a crossbeam for load distribution. Judging from the crack propagation at the ultimate state, as shown in Figure 14, the crack propagation in the case of a 28-day drying period seems to be affected by the eccentricity of the loading points, or the restriction on rotation or displacement caused by the loading or supporting points. As shown in Figure 15, for example, when the eccentricity of the loading point happens at one of the loading points, and the same amount of load is applied, the maximum moment generated in the beam is 4/3 times that in a beam loaded by four-point loading. Actually, this is a rare situation, but judging from the observed asymmetrical crack propagation, the beam dried for 28 days was somewhat affected by this eccentricity of the loading point, resulting in a lower flexural strength in the experiment.

5. SIZE EFFECT OF FLEXURAL STRENGTH CONSIDERING THE EFFECT OF INITIAL STRESS

Both test and analytical results are shown in Figure 16. The vertical and horizontal axes respectively indicate the ratio of flexural strength f_b to tensile strength f_t and specimen height h divided by the concrete characteristic length $l_{ch} = E_c G_F / f_t^2$ as a nondimensional number. Cases in which there is no initial stress, corresponding to cases in which specimens have been continuously cured in water, are indicated by ▲ and ● in Figure 16; cases in which specimens have been dried and initial stress exists are indicated by □, △, and ○.

The test results shown in Figure 16(a) for cases with no influence of initial stress indicate that the ratio of flexural strength to tensile strength f_b/f_t is on a single curve. Therefore, in this case, it is possible to use the parameter h/l_{ch} to determine f_b/f_t as an independent value without considering the age of concrete. However, in cases where initial stress exists due to drying shrinkage, despite the tendency of f_b/f_t to decrease as h/l_{ch} increases, (i.e. a significant size

effect is recognized), the magnitude of f_b/f_t itself changes with the drying period. As described in 4.3, this can be considered a combined action of the time-dependent change in initial stress distribution and material properties resulting from the progress of drying. Further, it is qualitatively clarified that the absence or presence of initial stress has a significant effect as h/l_{ch} increases, and that differences in the magnitude of f_b/f_t result from the absence or presence of initial stress.

Figure 16(b) shows the size effect through finite element analysis. In this analysis, the test results shown in Figures 10 and 11 are respectively used as the initial stress distribution due to drying shrinkage and for the time-dependent changes in material properties. The results of this size effect analysis more clearly show the effect of initial stress. In other words, when initial stress exists, it is possible to predict the size effect considering the effect of initial stress; further, as h/l_{ch} becomes larger, the influence of the absence or presence of initial stress is magnified.

Figure 17 compares values of flexural strength obtained from numerical analysis and from experiment; these values are nondimensionalized by tensile strength. Beam height, absence or presence of initial stress, and age differ according to test conditions. From Figure 17, the mean of analysis and test results is 0.984 and the coefficient of variance is 11.7%. It is thus confirmed that flexural strength can accurately be estimated through numerical analysis based on fracture mechanics, even if initial stress exists, by correctly evaluating the time-dependent changes in material properties and taking the magnitude and shape of the initial stress distribution into account.

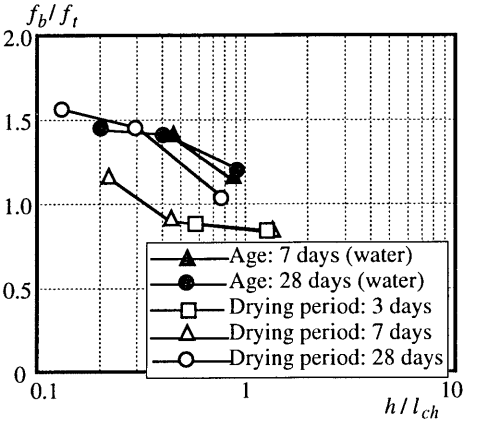

(a) Size effect obtained from tests

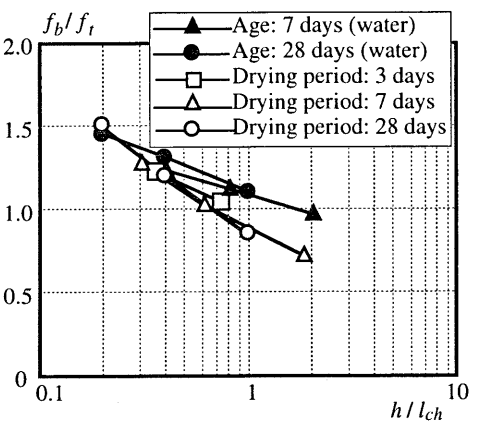

(b) Size effect obtained from analysis

Figure 16. Size Effect of Flexural Strength Considering Initial Stress Distribution

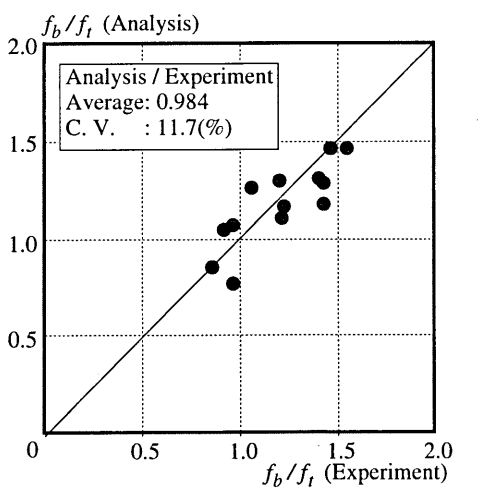

Figure 17. Comparison between Analysis and Experiment for Flexural Strength

6. CONCLUSIONS

This study was carried out to clarify the degree of influence that initial stress due to drying shrinkage has on the size effect of concrete flexural strength. As the basis for the study, the initial stress distribution was first measured and its shape was clarified through testing. Further, the time-dependent changes in material properties were studied. Finally, the size effect of flexural strength was predicted through numerical analysis based on the above-mentioned information, and was confirmed through tests. The following conclusions were reached:

(1) The initial stress distribution in concrete resulting from drying shrinkage changes with the size of the specimen and the drying period. With a small specimen and a sufficiently long drying period, the shape of the initial stress distribution can be modeled as a second-order polynomial curve. However, when the specimen is large and the drying period is short, it is not appropriate to assume that the initial stress distribution is a second-order polynomial curve.
(2) The compressive strength, elastic modulus, and fracture energy of concrete gradually increase as time passes, even when the concrete is dried. However, unlike the above properties, the tensile strength decreases gradually if the concrete is dried.
(3) The flexural strength of concrete beams with heights of 10 cm and 20 cm suddenly decreases at the initial stage of drying, later recovering gradually as the drying period increases. This behavior can be predicted through numerical analysis by adopting a proper distribution of initial stress and taking time-dependent changes in material properties into account.
(4) It was confirmed that initial stress due to drying shrinkage has an influence on the size effect of flexural strength. The influence of initial stress is significant in relatively large concrete beams with large h/l_{ch}. On the contrary, in small concrete beams with small h/l_{ch}, the effect of initial stress is not significant.

Acknowledgments

We wish to express our sincere gratitude to Professor Ikuo Hirasawa and the members of his laboratory at the Department of Civil Engineering of Chubu University for their cooperation in carrying out of this experiment.

References

[1] CEB, "CEB-FIP Model Code 1990", Bulletin d'Information, No. 213/214, 437 pp., 1993.
[2] Uchida, Y., Rokugo, K., and Koyanagi, W., "Application of Fracture Mechanics to Size Effect on Flexural Strength of Concrete", Journal of Materials, Concrete Structures and Pavements of JSCE, No. 442, V-16, pp. 101-107, 1992 (*in Japanese*).
[3] Hidaka, S., Niwa, J., and Tanabe, T., "Influence of Various Parameters on the Size Effect in the Flexural Strength of Concrete", Proceedings of the Japan Concrete Institute, Vol. 16, No. 2, pp. 33-38, 1994 (*in Japanese*).
[4] Tazawa, E., Miyazawa, S., Yamamoto, T., and Saito, K., "Self Stress due to Differential Drying Shrinkage of Plain Concrete", Proceedings of the Japan Concrete Institute, Vol. 10, No. 2,

pp. 255-260, 1988 (*in Japanese*).
[5] Akita, H., Fujiwara, T., and Ozaka, Y., "Shrinkage Stresses Derived from the Distributions of the Water Contents in Concrete Specimens", Proceedings of the Japan Concrete Institute, Vol. 13, No. 1, pp. 403-408, 1991 (*in Japanese*).
[6] Kawada, Y., et al.(ed.), "Stress Measurement Manual", OHM Co. Ltd., 1972.
[7] Niwa, J., "Size Effect Analysis on the Flexure Strength of Concrete Beams with Nonlinear Rod Element", Proceedings of the Japan Concrete Institute, Vol. 15, No. 2, pp. 75-80, 1993 (*in Japanese*).